No difference in local structure about a Zn dopant for congruent and stoichiometric LiNbO_{3}

F. Bridges, C. Mackeen, and L. Kovács

Is the local structure about a Zn dopant different for congruent and stoichiometric LiNbO$_3$?

F. Bridges,[1] C. Mackeen,[1] and L. Kovács[2]

[1]*Physics Department, University of California, Santa Cruz, California 95064, USA*
[2]*Institute for Solid State Physics and Optics, Wigner Research Center for Physics, Budapest, Hungary*
(Dated: June 15, 2016)

We compare EXAFS (extended x-ray absorption fine structure) data at the Zn K edge for a low concentration of Zn (0.7 mol%) in a stoichiometric crystal with that for higher Zn concentrations (nominally 5 and 9 mol%) in congruent LiNbO$_3$ (LNO). Note that stoichiometric and congruent LNO have significantly different optical properties. We find no significant difference in the local structure about Zn out to 4 Å for the two types of crystals and different dopant levels. Although some earlier theoretical models suggest a self compensation model with 75 % of Zn on a Li site and 25 % Zn on Nb, we find no clear evidence for a significant fraction of Zn on the Nb site, and estimate at most 2-3 % of Zn might be Zn$_{Nb}$.

I. INTRODUCTION

LiNbO$_3$ (LNO) is used in a wide range of acoustic and optical applications because of important properties such as large piezoelectric, acousto-optic, photoconductive, ferroelectric, photorefractive, and non-linear optical parameters[1]. For second harmonic generation, high intensity light is needed - but this leads to optical damage in materials with a large photorefractive response. For LNO, adding dopants such as Zn, Mg, In, etc. suppresses the photorefractive response, making the material much more resistant to optical damage[2,3]. In order to model mechanisms for photorefraction suppression, the dopant site(s) needs to be determined and the extent of distortion about them measured.

LNO crystalline material is produced in two forms. The most common is congruent LNO (cLNO, approximately Li$_{0.95}$Nb$_{1.01}$O$_3$) which has excess Nb plus vacancies on the Li sites; it has been studied for decades and is used in a range of optical applications. In contrast stoichiometric LNO (sLNO) has only been synthesized relatively recently and it's optical properties can differ significantly from cLNO as discussed in a recent review article[4]. For example, sLNO is more optical damage resistant (ODR) than cLNO, and the threshold concentration for divalent ions that enhance ODR is much lower - close to 0 mol%, in contrast to the threshold for cLNO, $\sim$ 5 mol%[4]. Also, Raman spectra are very different for the two types of crystals, and similarly for OH$^-$ vibration modes from very dilute OH$^-$ impurities. For the latter, a sharp narrow line is observed in sLNO, but a very broad band for cLNO. Finally, sLNO is much harder to dope with defect atoms than cLNO.

For congruent materials, Xu *et al.*[5] have calculated defect energies for a range of dopants but did not consider Zn explicitly; for other 2+ dopants, they found the lowest energy in congruent material to be for substitution on the Li site with neighboring Li vacancies – Zn$_{Li}$ + V$_{Li}$; however they did not consider a threshold dopant concentration. For material close to stoichiometric compositions, impurities may go onto both Li and Nb sites, but including the effects of intrinsic defects they concluded that the concentration of impurities on the Nb site would be negligible for stoichiometric material. In contrast for stoichiometric LNO (sLNO) at low Zn concentrations, Araujo *et al.*[6] found the lowest energy with the self compensating defect being Zn on a Nb site: i.e. $3Zn_{Li} + Zn_{Nb}$. Thus it is important to investigate the local structure about a given dopant atom in both types of crystals, and for different concentrations. Note also that the divalent Mg dopant is thought to change its environment above the photorefractive threshold, and this strongly depends on the stoichiometry. Below threshold Mg goes to the Li site, while above threshold it goes to the Nb site[7–9]. Xu *et al.*[5] arrived at a similar conclusion for Mg dopants from DFT calculations, with the dopant site depending on the chemical potential for Mg. In general Xu *et al.*[5] find that when the chemical potential corresponds to the stoichiometric material, the defect formation energies become positive, which leads to very low defect concentrations.

In an earlier study[10], we investigated the local structure in Zn doped congruent materials for a range of higher Zn concentrations using the EXAFS (extended x-ray absorption fine structure) technique, at both the Zn and Nb K edges. The environment about Zn was nearly identical for all Zn concentrations with a small increase in local disorder for the higher concentration samples. Detailed fits found that a Li site substitution model fit very well, with a small contraction of the O neighbors (compared to a Li site) and a slight expansion of the Nb shells. The signature of substitution on a Nb site would be a large (6 neighbors) Zn-Nb peak near 3.76 Å; that was not observed although a small concentration of Zn$_{Nb}$ could not be excluded. The environment about the Nb site (Nb EXAFS) was very consistent with diffraction experiments.

Here we report the EXAFS results at the Zn K edge for Zn doped stoichiometric material and show that the

environment about Zn is essentially the same as that observed previously for congruent material, with slightly less local disorder.

II. EXPERIMENTAL DETAILS

EXAFS data were collected at the Zn K edge in fluorescence mode, for Zn doped stoichiometric $LiNbO_3$, using beam line 4-1 at the Stanford Synchrotron Radiation Lightsource (SSRL). Data were collected at 10 K in an Oxford helium cryostat, using a 220 monochromator, with a slit size of 0.5 mm; energy resolution was 0.9 eV. Harmonic content was reduced by detuning the monochromator 50 % at 9800 eV. For the earlier work on cLNO, the energy resolution was 1.9 eV using a 111 monochromator[10].

The stoichiometric $LiNbO_3$ crystal doped with nominally 1 mol% ZnO was grown using the high temperature top seeded solution growth method with K_2O flux[4]. The Zn concentration in a different piece of sample, cut from the middle part of the crystal, was about 0.66 mol% as determined by atomic absorption spectrometry (AAS). The crystal was above the photorefractive damage threshold, checked by measuring the IR absorption spectrum of hydroxyl ions always present in as-grown LNO crystals[11]. A Zn concentration was also estimated from the Zn and Nb edge step heights for the EXAFS sample - 0.74 mol%. Considering the samples were from different parts of the boule, these results are consistent; we'll use the average concentration 0.7 mol%. We also re-measured concentrations in the earlier samples[10] as there was an error in converting x-ray step heights to relative concentrations; the correct concentrations are: 4.4 mol% (nom. 5 mol%); 5.3 mol% (nom. 7 mol%); 6.0 mol% (nom. 9 mol%); we use these in the later comparisons.

For the EXAFS experiments, a small amount of material was powdered and mounted on tape; the resulting particle sizes were ≤ 5 μm. Four layers of tape were loaded into the cryostat for the x-ray measurements. Details about the EXAFS technique are provided in our earlier study[10] – the procedures for the sLNO study are nearly identical to that work.

III. EXAFS DATA AND ANALYSIS

The fluorescence k-space data at 10K for the Zn K edge are plotted in Fig. 1:top for the stoichiometric sample (0.7 mol% Zn; black solid line) and for the congruent sample (4.4 mol% Zn, (nominal 5 mol%); red dotted line) from our earlier study[10]. Because of the poorer signal-to-noise at high k for the low concentration sLNO sample, the useful k-range only extends up to ~ 13.2 Å^{-1}. We therefore fit the background above the edge over a shorter range and for comparison purposes, used the same parameters to re-fit the background for the old data for cLNO. The
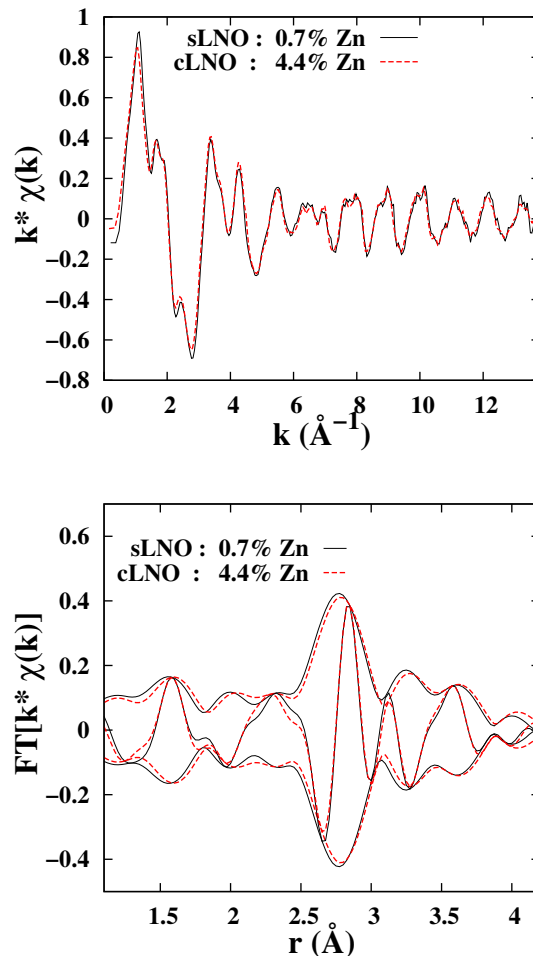

FIG. 1: (Color online.) Top: the k-space data for sLNO (0.7 mol% Zn) and cLNO (4.4 mol% Zn) samples; sLNO black line, cLNO red dashed line, at 10K. The data for sLNO have more noise at high k because of the much lower Zn concentration, and this limits the Fourier transform (FT) range. Bottom: Plot of the corresponding fast FT (FFT) of the k-space data with an FT window 3.8-13.2 Å^{-1}; the FT window is Gaussian rounded using a width, 0.2 Å^{-1}. There is a tiny difference between the data for sLNO and cLNO - the sLNO r-space plot has a slightly larger amplitude ($\sim 1\%$) for all Zn-Nb peaks, consistent with a lower dopant concentration. For the r-space data (here and in later plots), the fast oscillating function is the real part, R, of the FFT while the amplitude is $\pm\sqrt{R^2 + I^2}$ where I is the imaginary part of the FFT.

k-space plots in Fig. 1:top for the two crystalline forms (stoichiometric and congruent) are nearly identical.

The corresponding r-space data are shown in Fig. 1:bottom, using the Fourier transform (FT) range 3.8-13.2 Å^{-1}. Because the k-space data in the top panel show a large oscillation from about 1-3.5 Å^{-1}, much of which is in the XANES regime, the lower end of the FT window is therefore set at 3.8 Å^{-1}. Note again that this is a slightly shorter FT range than in the earlier study. In the r-space data the amplitude of the Zn-O peaks (1.5-2
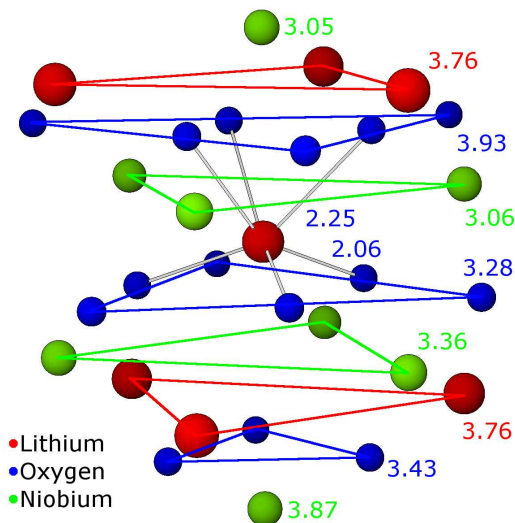
FIG. 2: (Color on-line) The environment about the central Li site (red) in LiNbO$_3$. Bonds are shown for the nearest O atoms; other O shells are shown as small (blue) atoms. The four green atoms (three in a plane) above the central atom are Nb at $\sim$ 3.06 Å; a second plane of Nb atoms is below the center at 3.36 Å, while the bottom Nb atom is 3.87 Å below center. There are six Li (red) neighbors (three above and three below center) at 3.76 Å.

Å) are nearly unchanged for the two samples, while the amplitudes of the three Zn-Nb peaks for sLNO (near 2.75, 3.25, and 3.65 Å) are slightly ($\sim$ 1%) larger. Other wise the position and shapes are nearly the same indicating essentially the same local environment.

The slight increase in amplitude for sLNO is to be expected since the Zn concentration is much lower and the average distortion in the lattice should be reduced. In particular, the Zn-Nb peak near 2.8 Å on the EXAFS plot, from four neighbors at $\sim$ 3.05 Å for a Li site occupation (Zn$_{Li}$), remains large for the sLNO sample; it is too large for 25% of the total Zn to be on the Nb site, as Zn$_{Nb}$ has no Zn-Nb peak near this distance.

Because the two r-space traces in Fig. 1:bottom are nearly identical in shape, the sLNO data were fit in the same way as the cLNO data[10], assuming Zn is primarily on a Li site. In this fit the number of neighbors were fixed to the coordination numbers about the Li site as determined from diffraction[12–14]; the initial environment and pair-distances (from diffraction) are shown in Fig. 2. In the fits we varied the pair distances and the width, σ, of the (Gaussian) pair distribution function for each peak. Initially we used the following peaks (with actual distances): two Zn-O peaks near 2.06 and 2.26 Å; three Zn-Nb peaks near 3.06, 3.36 and 3.87 Å, and a longer Zn-O peak near 3.29 Å. From our earlier study the Zn-O peaks at 3.28 and 3.43 Å could not be resolved (and appeared to move together). Several weaker peaks are also included - a long Zn-O peak ($r \sim$ 3.93 Å), a weak Zn-Li peak ($r \sim$ 3.76 Å), and two weak multi-scattering

TABLE I: Fit results for the Zn K edge data at 10K, for the sLNO (0.7 mol%) and cLNO (4.4 mol%; nominal 5 mol%) samples, plus distances from diffraction (Diff.). The Zn-O3 shell represents two longer Zn-O shells (three neighbors each at 3.28 and 3.43 Å; which collapse to a single peak with six O neighbors at an average distance near 3.25 Å. The second column gives corresponding pair distances about the Li site from diffraction for congruent LiNbO$_3$. The errors for r are $\pm$ 0.01 Å for the major peaks and most relative errors for σ^2 are $\pm$ 0.0005 Å^2. However systematic errors in σ^2 can be $\sim$ 10 %.

LiNbO$_3$	Diff.	cLNO (4.4 mol%)		sLNO (0.7 mol%)	
Atom pair	r (Å)	r (Å)	σ^2 (Å^2)	r (Å)	σ^2 (Å^2)
Zn-O1	2.06	2.01	0.0050	2.01	0.0049
Zn-O2	2.26	2.25	0.0083	2.24	0.0079
Zn-Nb1	3.06	3.13	0.0032	3.12	0.0028
Zn-O3	–	3.24	0.0037	3.24	0.0052
Zn-Nb2	3.36	3.38	0.0033	3.38	0.0033

(MS) peaks (Zn-O-Nb and Zn-O-O).

The r-space fit range for both samples was 1.3 - 4.3 Å and an example of a fit is shown in Fig. 3 for the sLNO sample; the individual peaks are shown below the fit and the weak peaks are show in an expanded window at the bottom of the figure. Not that the two MS peaks are nearly out of phase (real part of FT) for most of the peak, and don't contribute much to the overall amplitude. The pair distances and σ^2 values from the fit for the sLNO sample are tabulated in Table I for the main peaks, along with corresponding results for the new fit of the 4.4 mol% Zn, cLNO sample. For the latter the distances for the main peaks, obtained over the slightly different k-range are nearly identical (within 0.01 Å) to the earlier work[10]; the only significant difference is for the weak Zn-O3 peak (an average of 2 peaks) that is slightly shorter by 0.05 Å in these fits. There are also small differences in the values of σ^2 between the new fit and the earlier results, but again the largest effects are for the weak Zn-O3 peak. A comparison between the cLNO and SLNO results in Table I show that the parameters for the two samples are nearly identical - the distances for the strong peaks agree to 0.01 Å or less and the σ^2 values agree within 5 %; for the more distant Zn-O3 and Zn-Nb2 the differences are slightly larger. As observed previously the O shells shift slightly towards the Zn while the Nb atoms move slightly away.

The above fit, assuming only a Li substitution site, fits the data very well. To explore how much Zn might be on the Nb site, we allowed a small occupation on this site; Zn$_{Nb}$ would add a relatively large Zn-Nb peak near 3.4-3.5 Å in the EXAFS plot (actual distance $\sim$ 3.76 Å) because there are 6 Nb neighbors at this distance about the Nb site. Also, the Zn-Li peaks for this site are small and can be neglected compared to the Zn-Nb peak. In addition the amplitude (i.e. number of neighbors) of the large peaks near 2.8 and 3.3 Å on Fig. 3 for Zn$_{Li}$ must
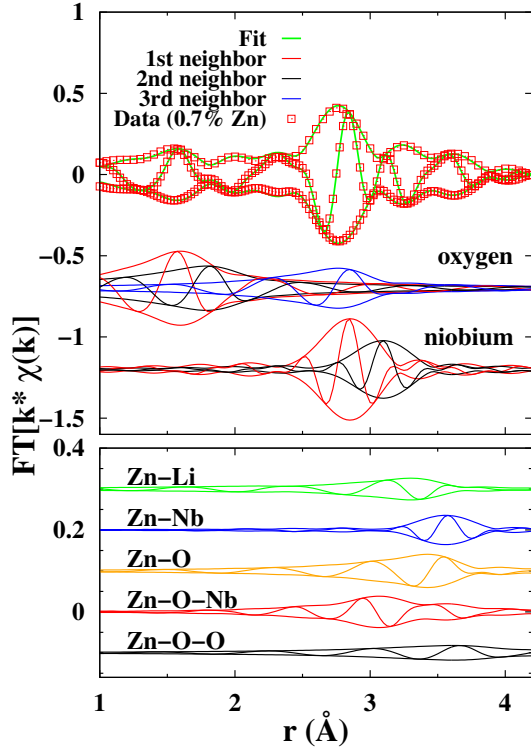
FIG. 3: A fit (solid line) of the Zn K edge data (squares) for sLNO with 0.7 mol% Zn, to a sum of functions calculated using FEFF[15]; the r-space fit range was 1.3-4.3 Å, and the FT range was 3.8-13.2 Å^{-1}; remaining degrees of freedom, 4. The fit is excellent over the entire fit range, particularly near 3.5 Å where a large Zn-Nb peak would exist if significant Zn were on the Nb site. The main individual peaks are plotted beneath the fit; the weak peaks for more distant neighbors – and also two MS peaks – are shown in an expanded view (zoomed by 2.5) in bottom panel.

decrease by the fraction on the Nb site. The fit does not want a peak at the expected position for Zn_{Nb} and rapidly becomes poor if a significant fraction of the Zn is on the Nb site; fits can be achieved with up to 6-7 % of the Zn on Nb, by varying σ and allowing a rather large increase in r. However the goodness-of-fit parameter only increases slightly; although there are more parameters, by using the Hamilton F-test,[16] this peak is not significant. Thus 6-7 % of the Zn is much too large an estimate for a Nb site occupation.

An additional problem with this fit is that it requires a large increase in the Zn-Nb distance for this extra peak, by nearly 0.1 Å; then it overlaps another Zn-Nb peak (Zn_{Li}) near $\sim$ 3.87 Å. Two unresolved peaks at nearly the same distance is not a reasonable model. From the fits to the Zn_{Li} site there is relatively little distortion about the defect for the distant neighbors beyond $\sim$ 3.8 Å – observed shifts in r are $\leq$ 0.02 Å for these long pair-distances. Also note that when divalent Zn replaces Li,

the closest O atoms are pulled in slightly while the nearer metal atoms are pushed away. On the other hand, for divalent Zn on the Nb(+5) site the reverse might be expected – O atoms relax slightly away from Zn while metal atoms move slightly inward. In any case one would not expect a large increase in a metal-pair distance this far from the Zn atom on a Nb site. We therefore carried out a fit starting with the best fit parameters for the Zn_{Li} site fit, plus a small Zn-Nb peak for some Zn on Nb (r $\sim$ 3.76 Å), but constrained any shift in r to be $\leq$ 0.02 Å. This fit suppresses the amplitude of the Zn-Nb peak for the Nb site - the amplitude decreases and the width increases such that on the scale of Fig. 3 this peak has little amplitude. This fit sets an upper limit of 2 % of the total Zn on the Nb site.

We also re-analyzed the data for the congruent samples (4.4 and 6.0 mol% Zn) using the above model and obtained the same result - if r is constrained to be $\leq$ 0.02 Å, the fraction of Zn on a Nb site is less than 2 %.

The difficulty in adding a Zn-Nb peak for the Zn_{Nb} site, close to the expected position (3.76 Å) can be observed visually assuming a somewhat higher concentration on the Nb site – e.g. assume a 10 % occupancy. The Zn-Li peaks are all small and the r-space plot is dominated by the long Zn-Nb peak for this site. In Fig. 4 we focus on the region from 3-4 Å, and compare the full fit of the data in Fig. 3 (well modeled by a Li site occupation) to a sum of the small Zn-Nb peak corresponding to 10 % Zn_{Nb} plus 90 % of the fit to the Zn_{Li} site; this sum is shown as a red line. The main issue is the change in shape of the real part R of the transform near 3.4-3.5 Å on the EXAFS plot. The fit for a Li site (and the data) have a clear kink in R near 3.4 Å; but with 10 % occupation on the Nb site the kink completely disappears, the shape of R becomes more symmetric, and the overall peak in R, shifts down to about 3.5 Å.

Optical damage resistance is increased in LNO crystals when the concentration of a suitable dopant (e.g. Zn, Mg, In, etc.) exceeds the so called threshold value, which depends on the valence state of the dopant, the stoichiometry of the crystal, and likely the substitution site. The higher the Li/Nb ratio the lower the threshold concentration[4]. For stoichiometric samples the threshold is close to 0 mol% while for congruent materials it is $\sim$ 5 mol% for divalent defects. While it is generally accepted that most of the dopants occupy Li sites in LNO crystals, the incorporation mechanism of the dopant may change above the threshold concentration[7] and some of the dopant might also occupy Nb sites[5–7].

Both cLNO and sLNO crystals containing optical damage resistant ions above the threshold, reveal an IR absorption band due to the stretching vibration of hydroxyl ions which form complexes with a dopant (e.g Zn) occupying the Nb site[11]. However, integrated absorption values per hydroxyl ions determined for LNO crystals[17] show that only very small amounts of the dopants are involved in such complexes and most of the dopant may still occupy Li sites in agreement with the present EX-
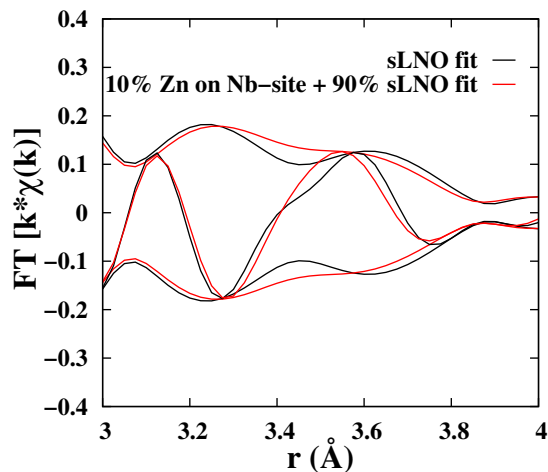
FIG. 4: The effect on the EXAFS plot if a small Zn-Nb peak with an actual distance of 3.76 Å, corresponding to 10 % Zn on the Nb site, is added to 90 % of the fit to the Li site. This adds a peak near 3.4-3.5 Å on the EXAFS plot, and even for this small amount of Zn on Nb, the shape of the real part of the transform, R, is changed significantly.

AFS results. As noted earlier, Xu *et al.*[5] argue that as the chemical potential moves towards that for the stoichiometric composition, the formation energy for 2+ defects becomes positive and further increases in dopant concentrations will be small. Thus although there may be a change in the doping mechanism (from $Zn_{Li} + 3\,V_{Li}$ to $Zn_{Nb} + 3\,Zn_{Li}$) as the Zn concentration exceeds the threshold composition, the net fraction of Zn_{Nb} may remain small. The strongest constraint should come from the sLNO sample but one cannot easily estimate the effective threshold concentration for a given crystal. The lack of a significant fraction of Zn_{Nb} for sLNO may suggest that the self compensating doping model ($Zn_{Nb} + 3\,Zn_{Li}$) may be suppressed. For congruent material, to have ~ 10 % of the Zn as Zn_{Nb} (which would be easily observable in EXAFS) as a result of a transition to the self compensating doping model above threshold, the concentration in the crystal would need to be about 9 mol% (4 mol% above the threshold concentration for divalent defects); then ~ 1 mol% would be Zn_{Nb}.

To summarize we have determined the local environment about Zn in stoichiometric LNO, using a low Zn concentration, 0.7 mol%. The environment is nearly identical to that for congruent LNO, but with slightly less local disorder - which is expected for a dilute impurity. The types of neighbors about Zn and distances to them indicate a primary Zn_{Li} site as found in the earlier study of Zn-doped congruent LNO. Thus the dominant substitution mechanism is $Zn_{Li} + 3\,V_{Li}$. However one must also include significant local distortions for the first few shells; on average, the O shells move towards Zn while the Nb shells move away. Such distortions will likely modify the energy calculations and there is likely a distribution of slightly different clusters about each Zn atom. Because of the positive defect formation energy for samples close to the stoichiometric composition[5] it is not clear that the Zn concentrations in sLNO can be increased sufficiently that a significant fraction of Zn_{Nb} (> 5 % of total Zn) are present.

[1] F. Xin, G. Zhang, F. Bo, H. Sun, Y. Kong, J. Xu, T. Volk, and N. M. Rubinina, J. Appl. Phys. **107**, 33113 (2010).

[2] X. Zhen, Q. Li, and Y. Xu, Cryst. Res. Technol. **41**, 276 (2006).

[3] U. Schlarb and K.Betzler, Phys. Rev. B **50**, 751 (1994).

[4] K. Lengyel, Á. Péter, L. Kovács, G. Corradi, L. Pálfalvi, J. Hebling, M. Unferdorben, G. Dravecz, I. Hajdara, Z. Szaller, and K. Polgár, App. Phys. Rev. **2**, 040601 (2015).

[5] H. Xu, A. Chernatynskiy, D. Lee, S. B. Sinnott, V. Gopalan, V. Dierolf, and S. R. Phillpot, Phys. Rev. B **82**, 184109/ (2010).

[6] R. M. Araujo, K. Lengyel, R. A. Jackson, L. Kovacs, and M. E. G. Valerio, J. Phys. Condes. Matt. **19**, 46211 (2007).

[7] B. Grabmaier, W. Wersing, and W. Koestler, J of Cryst. Growth **110**, 339 (1991).

[8] N. Iyi, K. Kitamura, Y. Yajijma, S. Kimura, Y. Furukawa, and M. Sato, J. Solid State Chem. **118**, 148 (1995).

[9] J. Liu, W. Zhang, and G. Zhang, Phys. Stat. Sol. (a) **156**, 285 (1996).

[10] F. Bridges, J. Castillo-Torres, B. Car, S. Medling, and M. Kozina, Phys. Rev. B **85**, 064107 (2012).

[11] L. Kovács, Z. Szaller, K. Lengyel, and G. Corradi, Opt. Mater. **37**, 55 (2014).

[12] S. C. Abrahams, J. M. Reddy, and J. L. Bernstein, J. Phys. Chem. Solids **27**, 997 (1966).

[13] S. C. Abrahams, H. J. Levinstein, and J. M. Reddy, J. Phys. Chem. Solids **27**, 1019 (1966).

[14] H. D. Megaw, Acta Cryst. A **24**, 583 (1968).

[15] A. L. Ankudinov, B. Ravel, J. J. Rehr, and S. D. Conradson, Phys. Rev. B **58**, 7565 (1998).

[16] L. Downward, C. H. Booth, W. W. Lukens, and F. Bridges, AIP Conference Proceedings **882**, 129 (2007).

[17] M. Wöhlecke and L. Kovács, Crit. Rev. Solid State Mater. Sci. **26**, 1 (2001).